



# The Tail of the Striatum: From Anatomy to Connectivity and Function

Emmanuel Valjent, Giuseppe Gangarossa

## ► To cite this version:

Emmanuel Valjent, Giuseppe Gangarossa. The Tail of the Striatum: From Anatomy to Connectivity and Function. Trends in Neurosciences, 2021, 44 (3), pp.203-214. 10.1016/j.tins.2020.10.016 . hal-03052590

**HAL Id: hal-03052590**

**<https://hal.science/hal-03052590>**

Submitted on 10 Mar 2023

**HAL** is a multi-disciplinary open access archive for the deposit and dissemination of scientific research documents, whether they are published or not. The documents may come from teaching and research institutions in France or abroad, or from public or private research centers.

L'archive ouverte pluridisciplinaire **HAL**, est destinée au dépôt et à la diffusion de documents scientifiques de niveau recherche, publiés ou non, émanant des établissements d'enseignement et de recherche français ou étrangers, des laboratoires publics ou privés.



Distributed under a Creative Commons Attribution - NonCommercial 4.0 International License

# **The Tail of the Striatum: from anatomy to connectivity and function**

Emmanuel Valjent<sup>1</sup> and Giuseppe Gangarossa<sup>2</sup>

<sup>1</sup>IGF, University of Montpellier, CNRS, INSERM, Montpellier, France

<sup>2</sup>Université de Paris, BFA, UMR 8251, CNRS, F-75013 Paris, France

Correspondence to: [giuseppe.gangarossa@u-paris.fr](mailto:giuseppe.gangarossa@u-paris.fr) (GG, [@PeppeGanga](#)) and  
[emmanuel.valjent@igf.cnrs.fr](mailto:emmanuel.valjent@igf.cnrs.fr) (EV)

**Keywords:** striatal heterogeneity; dopamine receptors; reward and aversive behaviors;  
psychostimulants; striatal projection neurons

## **Abstract**

The dorsal striatum, the largest subcortical structure of the basal ganglia, is critical in controlling motor, procedural and reinforcement-based behaviors. Although in mammals the striatum extends widely along the rostro-caudal axis, current knowledge and derived theories about its anatomo-functional organization largely rely on results obtained from studies of its rostral sectors, leading to potentially oversimplified working models of the striatum as a whole. Recent findings indicate that the extreme caudal part of the striatum, also referred to as the tail of striatum (TS), represents an additional functional domain. Here, we provide an overview of past and recent studies revealing that the TS displays a heterogeneous cell-type-specific organization and a unique input-output connectivity which poises the TS as an integrator of sensory processing.

## **The forgotten territories of the striatum**

The dorsal striatum is the main gateway of the basal ganglia, a group of subcortical nuclei which ensures motor control, action selection, decision making, as well as procedural and reinforcement-based learning [1–3]. In mammals, the striatum is primarily composed of GABAergic striatal projection neurons (SPNs) onto which converge glutamatergic projections from the entire cerebral cortex, thalamus and limbic regions including the hippocampus and amygdala. The multimodal signals conveyed by corticostriatal and thalamostriatal inputs are detected and integrated by SPNs [4]. The computed relevant information is in turn relayed to the output structures of the basal ganglia, thereby allowing the selection and execution of optimized motor sequences [5–8]. These filtering properties are also tightly modulated by monoaminergic signals conveyed by dopaminergic and serotonergic projections originating from the midbrain dopamine (DA) neurons and dorsal raphe nucleus, respectively [9,10].

Despite decades of research, the anatomo-functional organization of the striatum is far from being fully understood. This quest has been largely hampered by the lack of anatomical markers allowing the clear delimitation of territorial boundaries. To date, three major functional domains, dynamically interacting with each other, have been delineated according to the topographic organization of glutamatergic and monoaminergic projections: *i)* the sensorimotor domain comprising the dorsolateral striatum and involved in habit formations, *ii)* the associative domain corresponding to the dorsomedial striatum and important for driving goal-directed behavior, and *iii)* the limbic domain which mediates motivational and affective functions and extend to the ventral striatum [11–15]. Our current understanding of the anatomo-functional organization of striatal circuits has undoubtedly benefited from the delineation of these domains. However, these distinct territories have been defined based on differences spanning across the mediolateral and dorsoventral axes of the rostral striatum. The absence of additional functional domains is somehow surprising since the striatum extends

along the rostro-caudal axis in mammalian brains. Interestingly, recent studies have started providing new insights into the organization of striatal circuits, supporting the existence of at least a fourth striatal functional domain located in the extreme caudal part of the dorsal striatum, also known as the tail of striatum (TS) (**Figure 1**). Here, we summarize key evidence revealing the peculiar anatomo-functional organization of the TS as characterized, among other features, by the non-random spatial distribution of SPNs-expressing dopamine D1 and D2 receptors (D1R-SPNs and D2R-SPNs). We also discuss the high responsiveness of signaling pathways in TS SPNs to psychostimulants. Finally, we review recent findings supporting the role of the TS in guiding appetitive and aversive behaviors relying on the processing of visual and auditory information.

## **Characterizing the TS by its connectivity**

### *Excitatory afferents*

The term “tail of the striatum” (TS) was early attributed to the rat striatal domain receiving cortical projections from the visual cortex [16]. Subsequently, detailed characterization of rodents’ cortical afferents projecting to the TS identified the sensorimotor, visual, and auditory cortices as the main sources of TS-projecting neurons [17]. These pioneering observations have been recently confirmed, and further extended, by large-scale projectome studies, whose advanced analyses have precisely redefined the corticostriatal connectivity throughout the rostro-caudal extension of the striatum, including the TS [18–22]. Additional inputs arising from the agranular/granular/dysgranular insular cortices, frontal and temporal association cortices, motor cortex and ecto/peri/entorhinal cortices have been recently described, thus refining the corticostriatal projections map within the TS [18–21] (**Figure 1**). Beyond corticostriatal afferents, inputs from distinct subcortical structures including the amygdala, subiculum, claustrum and endopiriform nucleus also converge into the TS,

suggesting that multisensory processing is likely to occur in the TS [19,20] (**Figure 1**). The degree of convergence into the TS of the aforementioned inputs is however not shared by all mammals. For instance, the caudate tail and posterolateral putamen in cats or macaque monkeys receive almost exclusively excitatory inputs from the visual cortex [23,24]. These observations suggest that the anatomo-functional organization of corticostriatal projections tends to be more segregated throughout the rostro-caudal axis in species in which the dorsal striatum has anatomically demarcated caudate and putamen nuclei.

Although thalamostriatal afferents are evolutionary more ancient than corticostriatal projections, the role of this excitatory network has been for a long time overlooked [25,26]. The analysis of large tracing datasets has recently provided a detailed map of thalamostriatal afferents innervating the rodents' dorsal striatum, including the TS [19,20]. Thus, thalamic nuclei, including the lateral and medial geniculate nuclei, the lateral and ventral posterior nucleus, the parafascicular and posterior intralaminar nuclei, represent the principal sources of thalamic inputs into the TS [19,20,27,28] (**Figure 1**). Interestingly, a similar pattern of connectivity has also been described in the brain of cats, tree shrews and non-human primates [29–32].

#### *Monoaminergic afferents*

The functional domains of the striatum receive massive projections from three segregated clusters of DA neurons located in the midbrain [33]. The ones arising from the substantia nigra *pars compacta* (SNc, or A9 group) primarily project to the dorsal striatum, whereas those originating from the retrorubral field (RrF, or A8 group) and the ventral tegmental area (VTA, or A10 group) mainly innervate the ventral striatum [34]. Within these clusters, molecularly-defined SNc and VTA DA neurons displayed biased projections along the rostrocaudal, mediolateral and dorsoventral axes of the DS [33]. Thus, while DA neurons

located to the ventral and dorsal tier of the SNc project massively to the lateral and the ventromedial part of the rostral and intermediate DS, respectively, TS-projecting DA neurons arise almost exclusively from the substantia nigra *pars lateralis* (SNpl) [33,35–37]. Similarly, DA neurons projecting to the tail of the caudate nucleus (CDt) in cats or monkeys are preferentially located in SNpl, thus revealing that the topographic organization of DA innervation is highly conserved in mammal brains [38,39] (**Figure 1**). Advances in the development of cell-type-specific trans-synaptic tracing methods have allowed to establish a comprehensive cartography of the connectivity of TS-projecting DA neurons [36]. Interestingly, unlike DA neurons innervating rostral sectors of the dorsal striatum, TS-projecting DA neurons receive a specific set of monosynaptic inputs from the globus pallidus, zona incerta, parasubthalamic and subthalamic nuclei, entopeduncular nucleus and SNr [36]. The peculiarity of TS-projecting DA neurons is also supported by their unique molecular signature characterized by the co-expression of the vesicular glutamate transporter 2 (VGLUT2) and the lack of dopamine D2 autoreceptors [33,35,37,40]. These neurochemical features reveal that TS-projecting DA neurons *i*) may co-release DA and glutamate and *ii*) may use other mechanisms than D2R to control the timing and the amount of DA released from presynaptic terminals. Although less characterized, serotonergic (5-HT) innervation from the dorsal raphe nucleus (DRN) has also been described in the TS of rodents as well as in the caudate nucleus of monkeys, thus constituting a second important source of neuromodulation [20,41] (**Figure 1**).

### *TS efferents*

TS-output neurons, which consist of SPNs, are segregated into two distinct populations projecting either to the caudal part of the external globus pallidus (GPe) (iSPNs) or to the Ep/GPi and SNr (dSPNs) (**Figure 1**). In the latter, striatal projections arising from the TS are

topographically organized as longitudinal lamina located in the ventral SNr extending from its medial and to its lateral part and comprising the *pars lateralis* [17]. Cell-type-specific tracing tools have been again determinant in defining the circuits controlled by TS SPNs. Thus, TS-output neurons establish monosynaptic contacts with DA neurons located in the SNpl [42] as well as with GABAergic neurons of the lateral SNr [43]. This latter population, which projects to motor thalamic nuclei innervating the M1 and M2 motor cortices, supports the existence of open motor loops that might explain how striatal sub-regions involved in sensory processing modulate and tune motor control outputs [43]. Importantly, anatomical and electrophysiological investigations in the primate CDt have indicated a similar efferent organization for CDt-output dSPNs and iSPNs [44–46], even though a small percentage of traced CDt SPNs (~15%) projected to both caudal SNr and GPe [45].

#### **Delineation of the rodent's TS by its unique cellular architecture**

The quest for anatomical markers allowing the delimitation of the TS has only begun. The use of transgenic mice expressing reporters (fluorescent proteins, epitope-tagged proteins, Cre recombinase) driven by specific promoters enables the delimitation of TS domains (**Table 1**). Based on the differential distribution of SPNs expressing either D1R or D2R or both, our group has recently proposed the existence of at least three TS domains: *i*) a D2R/A2aR-SPNs-lacking domain, *ii*) a D1R- and D2R/A2aR-SPNs-intermingled domain and *iii*) a D1R/D2R-SPNs-coexpressing domain [47].

#### *The D2R/A2aR-SPNs-lacking domain*

In the course of our attempt of characterizing the spatial distribution of D1R- and D2R-SPNs throughout the rostro-caudal axis of the striatum, we have uncovered in the TS the existence of a longitudinal stripe adjacent to the GPe comprising D1R-expressing SPNs exclusively

[35,47]. The absence of D2R/A2aR-SPNs was further supported by the lack of expression of specific markers of this SPN population including D2R, A2aR, enkephalin, Gpr6 and 5'-nucleotidase [48–51]. To date, this represents the best cellular hallmark of this first TS domain which most likely corresponds to the medial part of the TS tri-laminar zone recently described [47,50] (**Figure 2**). The D2R/A2aR-SPNs-lacking domain is also identifiable by a dense plexus of fibers immunoreactive for substance P [35,50], reminiscent of the one described in the “marginal division” (MrD) [52]. However, the lack of  $\mu$  opioid receptor (MOR) and enkephalin immunoreactivities in D2R/A2aR-SPNs-lacking domain compared to the MrD indicates that they may not be one and the same caudal domain [35,50,52].

Local GABA- and ACh-releasing interneurons, which represent ~5% of striatal neurons, play a fundamental role in governing the activity and functions of the striatum [53–55]. Beside the peculiar spatial arrangement of D1R-SPNs and D2R-SPNs, a differential distribution of NOS- and ChAT-containing interneurons has been observed in the mouse TS [50]. This cellular feature is of interest, since striatal ChAT interneurons are generally characterized by the co-expression of D2R [56]. In fact, whereas ~94% of ChAT interneurons co-expressed GFP in the dorsal striatum of *Drd2*-eGFP mice, such percentage dropped down to ~17% in the D2R/A2aR-SPNs lacking domain of the TS [35], thereby highlighting a further cellular heterogeneity along the rostro-caudal striatal axis. Importantly, via local cell-to-cell communication, D2R-SPNs and ChAT interneurons are known to modulate the activity of D1R-SPNs [57–62]. Recently, by implementing experimental data with *in silico* modeling, it has been estimated that D2R-SPNs show higher probability to form synaptic contacts with SPNs (both D1R-SPNs and D2R-SPNs) than D1R-SPNs [61,63,64]. Interestingly, the virtual absence of D2R-SPNs and the low percentage of ChAT/D2R-positive interneurons in the TS D2R/A2aR-SPNs lacking domain indicate that D1R-SPNs

may possess unique physiological properties (reduced inhibitory drive) that indeed require further mechanistic and functional investigations.

#### *The D1R- and D2R/A2aR-SPNs-intermingled domain*

Adjacent to the D2R/A2aR-SPNs-lacking domain, we have identified a D1R- and D2R/A2aR-SPNs-intermingled domain which extends laterally throughout the dorso-ventral axis of the TS [47]. This domain has been further subdivided into two zones corresponding to the intermediate and lateral parts of the tri-laminar zone, respectively [50]. Despite their recent description, up to ten markers can be used to delineate these two zones (**Figure 2, Table 1**). The intermediate zone displays an ovoid shape easily identifiable by the low expression of TH- and DAT-containing fibers [35,47,50]. This zone is also characterized by low levels of D1R and high expression of D2R/A2aR consistent with reduced number of D1R-SPNs compared to D2R/A2aR-SPNs [47,50]. The lateral zone is delineated by an intense enkephalin labeling and a high PKC $\gamma$  expression [50] (**Figure 2**). Interestingly, corticostriatal sensory projections innervating these two zones are highly segregated. Indeed, the intermediate zone receives excitatory inputs from the auditory cortex, whereas the lateral zone is preferentially innervated by the agranular insular cortex [21]. All these anatomical features, which are highly conserved across the *Muridae* family (mouse, rat, gerbil), suggest that this topographic organization may have functional consequences by compartmentalizing the sensory-related processes integrated and relayed by the TS [47].

#### *D1R/D2R-SPNs-coexpressing domain*

The third TS domain lies between the central amygdala (CeA), and the D1R- and D2R/A2aR-SPNs-intermingled domain [47]. This domain is characterized by a proportion of D1R/D2R-coexpressing SPNs (~33%, [47]) much higher than that reported in the dorsal and ventral

regions of the rostral striatum, thus constituting one of its main anatomical features [35,47,65–69]. This domain most likely corresponds to the amygdalo-striatal transition area (AST), which processes, together with the adjacent CeA, emotionally relevant information (**Box 1**).

### **Hyper-responsiveness of TS neurons to psychostimulants**

Over the past decades, the analysis of DA-evoked molecular signaling events, such as the post-translational modifications (phosphorylation) of ERK, histone H3, and ribosomal protein S6 (rpS6), have been commonly used as molecular readouts for monitoring the activation of SPNs in response to appetitive, aversive and pharmacological stimuli [70]. This approach has provided the first insights into the differential functions of the TS domains.

The activation of SPNs in the TS was first described in response to systemic administration of the D1R agonist SKF81297 [71]. Topographic and cell-type-specific analyses indicated that ERK, histone H3, and rpS6 phosphorylations were specifically enhanced in D1R-SPNs located in TS zones processing visual and auditory information [71]. According to the recently proposed delineation of TS territories, the phosphorylation of ERK was restricted to the D2/A2aR-SPNs-lacking domain (medial zone) and the lateral and dorsal parts of the D1R- and D2R/A2aR-SPNs-intermingled domain [47]. Similar patterns of DA-dependent ERK, histone H3 and rpS6 phosphorylation were observed after acute administration of d-amphetamine, methamphetamine, cocaine, methylphenidate, 3,4-methylenedioxymethamphetamine (MDMA) or GBR12783, a selective inhibitor of DA reuptake [47,72] (**Figure 3**). These DA-dependent signaling events, which occurred selectively in D1R-SPNs, depend on the stimulation/activation of D1R [47,72]. Interestingly, ERK activation in the TS appears to be selective for psychostimulants since other classes of drugs, such as hallucinogens (2,5-dimethoxy-4-iodoamphetamine, phencyclidine,

dizocilpine), antidepressants (desipramine, fluoxetine), antipsychotics (haloperidol, raclopride) or mood stabilizers (lithium), failed to trigger ERK activation [47]. Further studies are needed to determine whether this pattern of ERK activation is specific to psychostimulants or shared by other classes of drugs of abuse as it is the case in the shell of the nucleus accumbens and the extended amygdala [73].

Although D1R-mediated ERK, histone H3, and rpS6 phosphorylations require the activation of the cAMP/PKA pathway in both the rostral parts of the dorsal striatum and the TS, recent work indicates that the underlying molecular mechanisms might be different [47,72,74]. Several explanations may account for the potent ERK activation in the D1R-SPNs of the TS D2R/A2aR-SPNs-lacking domain compared to those of the antero-dorsal striatum [47]. Indeed, the absence of the tonic inhibition on ERK phosphorylation mediated by the collateral inhibition of D2R-SPNs onto D1R-SPNs of the medial zone could be one of them. In fact, the D1R-dependent ERK phosphorylation in the antero-dorsal striatum is enhanced in mice lacking D2R in D2R/A2aR-SPNs [75]. Moreover, evidence suggest that the inactivation of the cAMP/PKA signaling normally achieved by PDE1b, PDE10A and PDE4, three SPNs-enriched phosphodiesterases (PDEs) isoforms [76], might not be optimal. Indeed, the lack of PDEs activities in D1R-SPNs of the medial zone certainly account for the rapid and sustained cAMP-dependent phosphorylation of ERK, histone H3 and rpS6 observed in the TS compared to the rostral sectors of the dorsal striatum [35,47,71] (**Figure 3**). Future studies are needed to determine whether D1R-SPNs of the TS D2R/A2aR-SPNs-lacking domain display unique molecular, physiological and functional features (**Figure 3, Box 2**).

### **The TS as an integrator of sensory processing**

Although the ability of TS SPNs to respond to a broad range of auditory stimulations has been established for decades [77], only recently the role of the TS in processing auditory

information has regained interest. Specifically, recent studies have demonstrated that the acquisition of a sound-driven discrimination task is accompanied by an enhanced auditory corticostriatal plasticity [78,79]. Consequently, inhibition of the auditory corticostriatal excitatory inputs, which tune information for striatum-dependent sound representations, impaired behavioral performance in an auditory frequency discrimination task [27]. It should be noted here that recently identified corticostriatal long-range inhibitory circuits might also contribute to the regulation of auditory processing [80,81]. Similarly, altered responses have been described following the inactivation of thalamostriatal inputs onto TS SPNs, thereby suggesting that both excitatory inputs are necessary to orchestrate auditory decision-making [27]. In addition, inactivation of TS D1R-SPNs impaired sound discrimination and the execution of behavioral tasks requiring auditory decisions [82]. Collectively, these studies support the key role of TS SPNs in integrating auditory sensory information with reward-associated signals to adjust and drive appropriate behavior [83]. A striking observation is that a transient auditory deprivation during development yields to persistent alterations in TS SPNs, thereby suggesting that the acquisition of their auditory-tuning properties might be permanently established during a brief developmental critical period [22]. This latter observation might explain the origin of striatal dysfunctions observed in sensory disorders associated with auditory processing [84,85]. Future studies will be essential in determining whether similar developmental mechanisms regulate the maturation of TS SPNs involved in visual information processing.

Reinforcement learning driven by visual and auditory stimuli relies in part on the ability of midbrain DA neurons to encode reward prediction error (RPE), salience and novelty [86–89]. Recent work indicates that TS-projecting DA neurons are functionally distinct from DA neurons innervating the dorsal and ventral sectors of the rostral striatum. Photometric  $\text{Ca}^{2+}$  recordings of DA axons have been determinant in demonstrating that TS-projecting DA

neurons are not only excited in response to novel cues but also by a variety of external sensory stimuli perceived as rewarding, aversive or neutral [90,91]. Their ability to convey general salient signals largely contribute to process reinforcement signals that promote avoidance of threatening stimuli [91]. Further studies are needed to precisely define whether reinforcement learning based on external threats engages distinct TS circuits depending on the nature and the anatomical sources of sensory stimuli (auditory, visual, somatosensory).

Some similarities may exist between the function of TS-projecting DA neurons in rodents and those projecting to the tail of the caudate (CDt) in primates. Indeed, midbrain DA neurons located in the dorsolateral part of the SNc are excited by both rewarding and aversive stimuli [88]. Importantly, these neurons, which also respond to salient visual stimuli, are thought to facilitate long-term memory of reward values of visual objects contributing to automatic and habitual saccades [92]. Importantly, at least two functionally distinct types of DA neurons have been highlighted in the primate SNc: the rostro-medial “update-type DA neurons” which, by mainly projecting to the caudate head (CDh), respond to unpredicted changes, and the CDt-projecting rostro-lateral “sustain-type DA neurons” which encode habitual behaviors [92]. Such functions might support a role of SPNs of the caudate tail in reward-driven visuomotor processing [93–95]. In line with the visual-related functions processed by the primate CDt, lesions of this striatal caudal region elicited an impairment of visual habit formation while sparing visual recognition memory [96]. In addition, neurons of the primate CDt, in opposition to the CDh, have been shown to selectively control automatic saccades-guided behavior when values of visual objects were more stable than flexible, the latter being dependent on the CDh [97]. Recently, taking advantage of optogenetic strategies, a role for CDt D1R-SPNs and D2R-SPNs has emerged as facilitators or suppressors of values-guided saccades, respectively [44,46]. However, whether sensory-related visual and/or auditory

stimuli are processed similarly in the TS/CDt of other species (i.e. human) remain to be fully established.

#### **Concluding remarks**

Parsing how the dorsal striatum is functionally organized has been largely hampered by the lack of anatomical markers allowing the clear delimitation of territorial boundaries. Current knowledge on striatal functions and dysfunctions is mainly built upon evidence obtained on rostral sectors of the striatum. However, recent data emerging from large-scale projectome studies have enabled refining the anatomo-functional organization of the dorsal striatum, thus suggesting that the TS may constitute a fourth striatal functional domain. Beyond a unique corticostriatal, thalamostriatal and nigrostriatal connectivity, recent findings indicate that, unlike in most rostral sectors of the dorsal striatum, segregated D1R- and D2R-SPNs are not randomly distributed in the rodents' TS. Future studies are needed to determine whether this key anatomical feature exists in other mammal species, including in non-human and human primate brains.

The existence of anatomically distinct TS domains raises questions about their functions. As mentioned above, the TS participates in encoding visual and auditory stimuli, thus representing a functional hub to allow sensory-associated reward, motor, aversive and decision-making functional outputs. However, how the TS territories and their cell-type components control such functional outputs remains to be established. The recent development of advanced methodologies combining rabies-mediated trans-synaptic tracing and Cre-based cell-type-specific targeting [98] will be valuable to precisely map monosynaptic inputs onto D1R- and D2-SPNs located in the distinct TS domains. Such anatomical characterization will be necessary to understand whether sensory (mainly visual and auditory) information is processed independently by each TS domain. Eventually, single-

326 cell gene expression profiling will enable defining whether molecular heterogeneity exists  
327 amongst TS SPNs that might help to better understand how information is computed in the TS  
328 to guide behaviors.

### **Box 1: The amygdalo-striatal transition area (AST)**

Despite its description more than four decades ago, the anatomo-functional organization of the amygdalo-striatal transition area (AST) in rodents and primates remains largely enigmatic [99–102]. Located between the TS and the central nucleus of the amygdala, adjacent to the caudal globus pallidus, the AST receives massive projections from visual and auditory thalamic centers as well as from the insula and amygdala nuclei [100,103–105]. The connectivity and cellular composition of the AST closely resembles those described for the dorsal striatum. Indeed, AST-output neurons segregate and project to the substantia nigra *pars lateralis* and caudoventral globus pallidus [100,106,107]. At the cellular and molecular levels, AST-output neurons comprise D1R-, D2R- and D1R/D2R-SPNs distributed in a random and equal proportion [47]. The AST is characterized by intense calretinin and angiotensin II immunoreactivities, two histological features shared with the extended amygdala [100,105]. Although early studies have suggested a role in the regulation emotional responses [106,108], future studies are required to determine whether salient events are integrated and processed at the level of the AST, and if so, how AST-output neurons contribute to guide motivated behaviors.

## **Box 2: Molecular and cellular heterogeneity within TS domains**

Recent methodological advances in gene expression profiling have unveiled an unexpected molecular heterogeneity among D1R- and D2R-SPNs throughout the dorso-ventral axis of the anterior striatum [56,109,110]. This molecular diversity appears to follow a specific spatial organization as illustrated by recent studies establishing spatio-molecular maps of SPNs in patch, matrix and exopatch compartments [111,112]. Interestingly, emerging evidence points to an additional level of molecular heterogeneity among SPNs throughout the striatal rostro-caudal axis, notably at the level of the TS. Indeed, the absence and/or inefficacy of SPNs-enriched PDEs or phosphatases in D1R-SPNs of the D2R/A2aR-SPNs-lacking TS domain may account for the sustained and enhanced phosphorylation events dependent on cyclic nucleotide signaling [47]. The molecular heterogeneity is not restricted to SPNs since only ~17% of the cholinergic interneurons located in the D2R/A2aR-SPNs-lacking domain express D2R [35]. This observation suggest that the diversity of striatal cholinergic interneurons is not restricted to the dorsoventral axis but also exist throughout the rostro-caudal axis [56,113]. Similar diversity may certainly exist in other striatal interneurons subtypes [114]. Finally, the use of barcoded anatomy resolved by sequencing (BARseq) [115] may provide important insights into the organizing principles underlying the anatomo-functional organization of TS circuits.

## **Acknowledgments**

We thank Denis Hervé and Jean-Antoine Girault for critical reading of the manuscript and for their insightful comments. This work was supported by Inserm, Fondation pour la Recherche Médicale (DEQ20160334919) (E.V.), La Marato de TV3 Fundacio (#113-2016) (E.V.), and Agence National de la Recherche (EPITRACES, ANR-16-CE16-0018; DOPAFEAR, ANR-16-CE16-0006) (E.V.), Université de Paris, Nutricia Research Foundation (G.G.), Allen Foundation Inc. (G.G.), Fyssen Foundation (G.G.).

## References

- 1 Hikida, T. *et al.* (2010) Distinct roles of synaptic transmission in direct and indirect striatal pathways to reward and aversive behavior. *Neuron* 66, 896–907
- 2 Kravitz, A.V. and Kreitzer, A.C. (2012) Striatal mechanisms underlying movement, reinforcement, and punishment. *Physiology (Bethesda)* 27, 167–177
- 3 Lee, D. *et al.* (2012) Neural basis of reinforcement learning and decision making. *Annu. Rev. Neurosci.* 35, 287–308
- 4 Wall, N.R. *et al.* (2013) Differential innervation of direct- and indirect-pathway striatal projection neurons. *Neuron* 79, 347–360
- 5 Peak, J. *et al.* (2019) From learning to action: the integration of dorsal striatal input and output pathways in instrumental conditioning. *Eur. J. Neurosci.* 49, 658–671
- 6 Hidalgo-Balbuena, A.E. *et al.* (2019) Sensory representations in the striatum provide a temporal reference for learning and executing motor habits. *Nat Commun* 10, 4074
- 7 Jin, X. and Costa, R.M. (2010) Start/stop signals emerge in nigrostriatal circuits during sequence learning. *Nature* 466, 457–462
- 8 Jin, X. *et al.* (2014) Basal ganglia subcircuits distinctively encode the parsing and concatenation of action sequences. *Nat. Neurosci.* 17, 423–430
- 9 Cavaccini, A. *et al.* (2018) Serotonergic Signaling Controls Input-Specific Synaptic Plasticity at Striatal Circuits. *Neuron* 98, 801–816.e7
- 10 Lerner, T.N. *et al.* (2015) Intact-Brain Analyses Reveal Distinct Information Carried by SNc Dopamine Subcircuits. *Cell* 162, 635–647
- 11 Balleine, B.W. and O'Doherty, J.P. (2010) Human and rodent homologues in action control: corticostriatal determinants of goal-directed and habitual action. *Neuropsychopharmacology* 35, 48–69
- 12 Thorn, C.A. *et al.* (2010) Differential dynamics of activity changes in dorsolateral and dorsomedial striatal loops during learning. *Neuron* 66, 781–795
- 13 Voorn, P. *et al.* (2004) Putting a spin on the dorsal-ventral divide of the striatum. *Trends Neurosci.* 27, 468–474
- 14 Gremel, C.M. and Costa, R.M. (2013) Orbitofrontal and striatal circuits dynamically encode the shift between goal-directed and habitual actions. *Nat Commun* 4, 2264
- 15 Floresco, S.B. (2015) The nucleus accumbens: an interface between cognition, emotion, and action. *Annu Rev Psychol* 66, 25–52
- 16 Donoghue, J.P. and Herkenham, M. (1986) Neostriatal projections from individual cortical fields conform to histochemically distinct striatal compartments in the rat. *Brain Res.* 365, 397–403
- 17 Deniau, J.M. *et al.* (1996) The lamellar organization of the rat substantia nigra pars reticulata: segregated patterns of striatal afferents and relationship to the topography of

407 corticostriatal projections. *Neuroscience* 73, 761–781

408 18 Hintiryan, H. *et al.* (2016) The mouse cortico-striatal projectome. *Nat. Neurosci.* 19,  
409 1100–1114

410 19 Hunnicutt, B.J. *et al.* (2016) A comprehensive excitatory input map of the striatum  
411 reveals novel functional organization. *Elife* 5,

412 20 Jiang, H. and Kim, H.F. (2018) Anatomical Inputs From the Sensory and Value  
413 Structures to the Tail of the Rat Striatum. *Front Neuroanat* 12, 30

414 21 Miyamoto, Y. *et al.* (2018) Striosome-based map of the mouse striatum that is  
415 conformable to both cortical afferent topography and uneven distributions of dopamine D1  
416 and D2 receptor-expressing cells. *Brain Struct Funct* 223, 4275–4291

417 22 Mowery, T.M. *et al.* (2017) The Sensory Striatum Is Permanently Impaired by  
418 Transient Developmental Deprivation. *Cell Rep* 19, 2462–2468

419 23 Updyke, B.V. (1993) Organization of visual corticostriatal projections in the cat, with  
420 observations on visual projections to claustrum and amygdala. *J. Comp. Neurol.* 327, 159–193

421 24 Seger, C.A. (2013) The visual corticostriatal loop through the tail of the caudate:  
422 circuitry and function. *Front Syst Neurosci* 7, 104

423 25 Smith, Y. *et al.* (2004) The thalamostriatal system: a highly specific network of the  
424 basal ganglia circuitry. *Trends Neurosci.* 27, 520–527

425 26 Reiner, A. *et al.* (2005) Organization and evolution of the avian forebrain. *Anat Rec A*  
426 *Discov Mol Cell Evol Biol* 287, 1080–1102

427 27 Chen, L. *et al.* (2019) Medial geniculate body and primary auditory cortex  
428 differentially contribute to striatal sound representations. *Nat Commun* 10, 418

429 28 Ponvert, N.D. and Jaramillo, S. (2019) Auditory Thalamostriatal and Corticostriatal  
430 Pathways Convey Complementary Information about Sound Features. *J. Neurosci.* 39, 271–  
431 280

432 29 Beckstead, R.M. (1984) A projection to the striatum from the medial subdivision of  
433 the posterior group of the thalamus in the cat. *Brain Res.* 300, 351–356

434 30 Day-Brown, J.D. *et al.* (2010) Pulvinar projections to the striatum and amygdala in the  
435 tree shrew. *Front Neuroanat* 4, 143

436 31 Galvan, A. and Smith, Y. (2011) The primate thalamostriatal systems: Anatomical  
437 organization, functional roles and possible involvement in Parkinson’s disease. *Basal Ganglia*  
438 1, 179–189

439 32 Harting, J.K. *et al.* (2001) Striatal projections from the cat visual thalamus. *Eur. J.*  
440 *Neurosci.* 14, 893–896

441 33 Poulin, J.-F. *et al.* (2020) Classification of Midbrain Dopamine Neurons Using Single-  
442 Cell Gene Expression Profiling Approaches. *Trends Neurosci.* 43, 155–169

443 34 Roeper, J. (2013) Dissecting the diversity of midbrain dopamine neurons. *Trends*

444 *Neurosci.* 36, 336–342

445 35 Gangarossa, G. *et al.* (2013) Spatial distribution of D1R- and D2R-expressing  
446 medium-sized spiny neurons differs along the rostro-caudal axis of the mouse dorsal striatum.  
447 *Front Neural Circuits* 7, 124

448 36 Menegas, W. *et al.* (2015) Dopamine neurons projecting to the posterior striatum form  
449 an anatomically distinct subclass. *Elife* 4, e10032

450 37 Poulin, J.-F. *et al.* (2018) Mapping projections of molecularly defined dopamine  
451 neuron subtypes using intersectional genetic approaches. *Nat. Neurosci.* 21, 1260–1271

452 38 Hontanilla, B. *et al.* (1996) A topographic re-evaluation of the nigrostriatal projections  
453 to the caudate nucleus in the cat with multiple retrograde tracers. *Neuroscience* 72, 485–503

454 39 Kim, H.F. *et al.* (2014) Separate groups of dopamine neurons innervate caudate head  
455 and tail encoding flexible and stable value memories. *Front Neuroanat* 8, 120

456 40 Yamaguchi, T. *et al.* (2013) Glutamate neurons in the substantia nigra compacta and  
457 retrorubral field. *Eur. J. Neurosci.* 38, 3602–3610

458 41 Griggs, W.S. *et al.* (2017) Flexible and Stable Value Coding Areas in Caudate Head  
459 and Tail Receive Anatomically Distinct Cortical and Subcortical Inputs. *Front. Neuroanat.*  
460 11,

461 42 Watabe-Uchida, M. *et al.* (2012) Whole-brain mapping of direct inputs to midbrain  
462 dopamine neurons. *Neuron* 74, 858–873

463 43 Aoki, S. *et al.* (2019) An open cortico-basal ganglia loop allows limbic control over  
464 motor output via the nigrothalamic pathway. *Elife* 8,

465 44 Amita, H. *et al.* (2020) Optogenetic manipulation of a value-coding pathway from the  
466 primate caudate tail facilitates saccadic gaze shift. *Nat Commun* 11, 1876

467 45 Amita, H. *et al.* (2019) Neuronal connections of direct and indirect pathways for stable  
468 value memory in caudal basal ganglia. *Eur. J. Neurosci.* 49, 712–725

469 46 Kim, H.F. *et al.* (2017) Indirect Pathway of Caudal Basal Ganglia for Rejection of  
470 Valueless Visual Objects. *Neuron* 94, 920-930.e3

471 47 Gangarossa, G. *et al.* (2019) Contrasting patterns of ERK activation in the tail of the  
472 striatum in response to aversive and rewarding signals. *J. Neurochem.* DOI:  
473 10.1111/jnc.14804

474 48 Harris, J.A. *et al.* (2014) Anatomical characterization of Cre driver mice for neural  
475 circuit mapping and manipulation. *Front Neural Circuits* 8, 76

476 49 Koshimizu, Y. *et al.* (2008) Paucity of enkephalin production in neostriatal striosomal  
477 neurons: analysis with preproenkephalin-green fluorescent protein transgenic mice. *Eur. J.*  
478 *Neurosci.* 28, 2053–2064

479 50 Miyamoto, Y. *et al.* (2019) Three divisions of the mouse caudal striatum differ in the  
480 proportions of dopamine D1 and D2 receptor-expressing cells, distribution of dopaminergic  
481 axons, and composition of cholinergic and GABAergic interneurons. *Brain Struct Funct* 224,

482 2703–2716

483 51 Schoen, S.W. and Graybiel, A.M. (1993) Species-specific patterns of glycoprotein  
484 expression in the developing rodent caudoputamen: association of 5'-nucleotidase activity  
485 with dopamine islands and striosomes in rat, but with extrastriosomal matrix in mouse. *J.*  
486 *Comp. Neurol.* 333, 578–596

487 52 Shu, S.Y. *et al.* (2003) New component of the limbic system: Marginal division of the  
488 neostriatum that links the limbic system to the basal nucleus of Meynert. *J. Neurosci. Res.* 71,  
489 751–757

490 53 Fino, E. *et al.* (2018) Region-specific and state-dependent action of striatal  
491 GABAergic interneurons. *Nat Commun* 9, 3339

492 54 Gritton, H.J. *et al.* (2019) Unique contributions of parvalbumin and cholinergic  
493 interneurons in organizing striatal networks during movement. *Nat. Neurosci.* 22, 586–597

494 55 Zucca, S. *et al.* (2018) Pauses in cholinergic interneuron firing exert an inhibitory  
495 control on striatal output in vivo. *Elife* 7,

496 56 Puighermanal, E. *et al.* (2020) Functional and molecular heterogeneity of D2R  
497 neurons along dorsal ventral axis in the striatum. *Nat Commun* 11, 1957

498 57 Czubayko, U. and Plenz, D. (2002) Fast synaptic transmission between striatal spiny  
499 projection neurons. *Proc. Natl. Acad. Sci. U.S.A.* 99, 15764–15769

500 58 English, D.F. *et al.* (2011) GABAergic circuits mediate the reinforcement-related  
501 signals of striatal cholinergic interneurons. *Nat. Neurosci.* 15, 123–130

502 59 Koos, T. *et al.* (2004) Comparison of IPSCs evoked by spiny and fast-spiking neurons  
503 in the neostriatum. *J. Neurosci.* 24, 7916–7922

504 60 Oldenburg, I.A. and Ding, J.B. (2011) Cholinergic modulation of synaptic integration  
505 and dendritic excitability in the striatum. *Curr. Opin. Neurobiol.* 21, 425–432

506 61 Taverna, S. *et al.* (2008) Recurrent collateral connections of striatal medium spiny  
507 neurons are disrupted in models of Parkinson's disease. *J. Neurosci.* 28, 5504–5512

508 62 Witten, I.B. *et al.* (2010) Cholinergic interneurons control local circuit activity and  
509 cocaine conditioning. *Science* 330, 1677–1681

510 63 Hjorth, J.J.J. *et al.* (2020) The microcircuits of striatum in silico. *Proc. Natl. Acad. Sci.*  
511 *U.S.A.* 117, 9554–9565

512 64 Planert, H. *et al.* (2010) Dynamics of synaptic transmission between fast-spiking  
513 interneurons and striatal projection neurons of the direct and indirect pathways. *J. Neurosci.*  
514 30, 3499–3507

515 65 Gangarossa, G. *et al.* (2013) Distribution and compartmental organization of  
516 GABAergic medium-sized spiny neurons in the mouse nucleus accumbens. *Front Neural*  
517 *Circuits* 7, 22

518 66 Gagnon, D. *et al.* (2017) Striatal Neurons Expressing D1 and D2 Receptors are  
519 Morphologically Distinct and Differently Affected by Dopamine Denervation in Mice. *Sci*

520 Rep 7, 41432

521 67 Wei, X. *et al.* (2018) Dopamine D1 or D2 receptor-expressing neurons in the central  
522 nervous system. *Addict Biol* 23, 569–584

523 68 Frederick, A.L. *et al.* (2015) Evidence against dopamine D1/D2 receptor heteromers.  
524 *Mol. Psychiatry* 20, 1373–1385

525 69 Rico, A.J. *et al.* (2017) Neurochemical evidence supporting dopamine D1–D2 receptor  
526 heteromers in the striatum of the long-tailed macaque: changes following dopaminergic  
527 manipulation. *Brain Struct Funct* 222, 1767–1784

528 70 Valjent, E. *et al.* (2019) Dopamine signaling in the striatum. In *Advances in Protein*  
529 *Chemistry and Structural Biology* Academic Press

530 71 Gangarossa, G. *et al.* (2013) Combinatorial topography and cell-type specific  
531 regulation of the ERK pathway by dopaminergic agonists in the mouse striatum. *Brain Struct*  
532 *Funct* 218, 405–419

533 72 Biever, A. *et al.* (2015) PKA-dependent phosphorylation of ribosomal protein S6 does  
534 not correlate with translation efficiency in striatonigral and striatopallidal medium-sized spiny  
535 neurons. *J. Neurosci.* 35, 4113–4130

536 73 Valjent, E. *et al.* (2004) Addictive and non-addictive drugs induce distinct and specific  
537 patterns of ERK activation in mouse brain. *Eur. J. Neurosci.* 19, 1826–1836

538 74 Polito, M. *et al.* (2015) Selective Effects of PDE10A Inhibitors on Striatopallidal  
539 Neurons Require Phosphatase Inhibition by DARPP-32. *eNeuro* 2,

540 75 Dobbs, L.K. *et al.* (2019) D1 receptor hypersensitivity in mice with low striatal D2  
541 receptors facilitates select cocaine behaviors. *Neuropsychopharmacology* 44, 805–816

542 76 Nishi, A. *et al.* (2008) Distinct roles of PDE4 and PDE10A in the regulation of  
543 cAMP/PKA signaling in the striatum. *J. Neurosci.* 28, 10460–10471

544 77 Bordi, F. and LeDoux, J. (1992) Sensory tuning beyond the sensory system: an initial  
545 analysis of auditory response properties of neurons in the lateral amygdaloid nucleus and  
546 overlying areas of the striatum. *J. Neurosci.* 12, 2493–2503

547 78 Znamenskiy, P. and Zador, A.M. (2013) Corticostriatal neurons in auditory cortex  
548 drive decisions during auditory discrimination. *Nature* 497, 482–485

549 79 Xiong, Q. *et al.* (2015) Selective corticostriatal plasticity during acquisition of an  
550 auditory discrimination task. *Nature* 521, 348–351

551 80 Rock, C. *et al.* (2016) An inhibitory corticostriatal pathway. *Elife* 5,

552 81 Bertero, A. *et al.* (2020) Auditory Long-Range Parvalbumin Cortico-Striatal Neurons.  
553 *Front Neural Circuits* 14, 45

554 82 Guo, L. *et al.* (2018) Stable representation of sounds in the posterior striatum during  
555 flexible auditory decisions. *Nat Commun* 9, 1534

556 83 Guo, L. *et al.* (2019) Choice-Selective Neurons in the Auditory Cortex and in Its

557 Striatal Target Encode Reward Expectation. *J. Neurosci.* 39, 3687–3697

558 84 Shepherd, G.M.G. (2013) Corticostriatal connectivity and its role in disease. *Nat. Rev.*  
559 *Neurosci.* 14, 278–291

560 85 Lim, S.-J. *et al.* (2019) Role of the striatum in incidental learning of sound categories.  
561 *Proc. Natl. Acad. Sci. U.S.A.* 116, 4671–4680

562 86 Cohen, J.Y. *et al.* (2012) Neuron-type-specific signals for reward and punishment in  
563 the ventral tegmental area. *Nature* 482, 85–88

564 87 Glimcher, P.W. (2011) Understanding dopamine and reinforcement learning: the  
565 dopamine reward prediction error hypothesis. *Proc. Natl. Acad. Sci. U.S.A.* 108 Suppl 3,  
566 15647–15654

567 88 Matsumoto, M. and Hikosaka, O. (2009) Two types of dopamine neuron distinctly  
568 convey positive and negative motivational signals. *Nature* 459, 837–841

569 89 Morrens, J. *et al.* (2020) Cue-Evoked Dopamine Promotes Conditioned Responding  
570 during Learning. *Neuron* 106, 142–153.e7

571 90 Menegas, W. *et al.* (2017) Opposite initialization to novel cues in dopamine signaling  
572 in ventral and posterior striatum in mice. *Elife* 6,

573 91 Menegas, W. *et al.* (2018) Dopamine neurons projecting to the posterior striatum  
574 reinforce avoidance of threatening stimuli. *Nat. Neurosci.* 21, 1421–1430

575 92 Kim, H.F. *et al.* (2015) Dopamine Neurons Encoding Long-Term Memory of Object  
576 Value for Habitual Behavior. *Cell* 163, 1165–1175

577 93 Yamamoto, S. *et al.* (2012) What and where information in the caudate tail guides  
578 saccades to visual objects. *J. Neurosci.* 32, 11005–11016

579 94 Yamamoto, S. *et al.* (2013) Reward value-contingent changes of visual responses in  
580 the primate caudate tail associated with a visuomotor skill. *J. Neurosci.* 33, 11227–11238

581 95 Hikosaka, O. *et al.* (2014) Basal ganglia circuits for reward value-guided behavior.  
582 *Annu. Rev. Neurosci.* 37, 289–306

583 96 Fernandez-Ruiz, J. *et al.* (2001) Visual habit formation in monkeys with neurotoxic  
584 lesions of the ventrocaudal neostriatum. *Proc. Natl. Acad. Sci. U.S.A.* 98, 4196–4201

585 97 Kim, H.F. and Hikosaka, O. (2013) Distinct basal ganglia circuits controlling  
586 behaviors guided by flexible and stable values. *Neuron* 79, 1001–1010

587 98 Sjulson, L. *et al.* (2016) Cell-Specific Targeting of Genetically Encoded Tools for  
588 Neuroscience. *Annu. Rev. Genet.* 50, 571–594

589 99 Alheid, G.F. *et al.* (1998) The neuronal organization of the supracapsular part of the  
590 stria terminalis in the rat: the dorsal component of the extended amygdala. *Neuroscience* 84,  
591 967–996

592 100 Shammah-Lagnado, S.J. *et al.* (1999) Afferent connections of the interstitial nucleus  
593 of the posterior limb of the anterior commissure and adjacent amygdalostratial transition area

594 in the rat. *Neuroscience* 94, 1097–1123

595 101 Cho, Y.T. *et al.* (2013) Cortico-amygdala-striatal circuits are organized as hierarchical  
596 subsystems through the primate amygdala. *J. Neurosci.* 33, 14017–14030

597 102 Fudge, J.L. and Tucker, T. (2009) Amygdala projections to central amygdaloid  
598 nucleus subdivisions and transition zones in the primate. *Neuroscience* 159, 819–841

599 103 Turner, B.H. and Herkenham, M. (1991) Thalamoamygdaloid projections in the rat: a  
600 test of the amygdala’s role in sensory processing. *J. Comp. Neurol.* 313, 295–325

601 104 Doron, N.N. and Ledoux, J.E. (1999) Organization of projections to the lateral  
602 amygdala from auditory and visual areas of the thalamus in the rat. *J. Comp. Neurol.* 412,  
603 383–409

604 105 Jolkkonen, E. *et al.* (2001) Interconnectivity between the amygdaloid complex and the  
605 amygdalostratial transition area: a PHA-L study in rat. *J. Comp. Neurol.* 431, 39–58

606 106 LeDoux, J.E. *et al.* (1990) The lateral amygdaloid nucleus: sensory interface of the  
607 amygdala in fear conditioning. *J. Neurosci.* 10, 1062–1069

608 107 Shammah-Lagnado, S.J. *et al.* (1996) Efferent connections of the caudal part of the  
609 globus pallidus in the rat. *J. Comp. Neurol.* 376, 489–507

610 108 Trogrlic, L. *et al.* (2011) Context fear learning specifically activates distinct  
611 populations of neurons in amygdala and hypothalamus. *Learn. Mem.* 18, 678–687

612 109 Gokce, O. *et al.* (2016) Cellular Taxonomy of the Mouse Striatum as Revealed by  
613 Single-Cell RNA-Seq. *Cell Rep* 16, 1126–1137

614 110 Saunders, A. *et al.* (2018) Molecular Diversity and Specializations among the Cells of  
615 the Adult Mouse Brain. *Cell* 174, 1015-1030.e16

616 111 Martín, A. *et al.* (2019) A Spatiomolecular Map of the Striatum. *Cell Rep* 29, 4320-  
617 4333.e5

618 112 Stanley, G. *et al.* (2020) Continuous and Discrete Neuron Types of the Adult Murine  
619 Striatum. *Neuron* 105, 688-699.e8

620 113 Virk, M.S. *et al.* (2016) Opposing roles for serotonin in cholinergic neurons of the  
621 ventral and dorsal striatum. *Proc. Natl. Acad. Sci. U.S.A.* 113, 734–739

622 114 Muñoz-Manchado, A.B. *et al.* (2018) Diversity of Interneurons in the Dorsal Striatum  
623 Revealed by Single-Cell RNA Sequencing and PatchSeq. *Cell Rep* 24, 2179-2190.e7

624 115 Chen, X. *et al.* (2019) High-Throughput Mapping of Long-Range Neuronal Projection  
625 Using In Situ Sequencing. *Cell* 179, 772-786.e19

626 116 Franklin, K. and Paxinos, G., K. The Mouse Brain in Stereotaxic Coordinates, 3rd  
627 Edn. . (2008), Elsevier

628 117 Gong, S. *et al.* (2003) A gene expression atlas of the central nervous system based on  
629 bacterial artificial chromosomes. *Nature* 425, 917–925

630

## Figure legends

### Figure 1: Delineating the tail of the striatum.

(a) Coronal view of the tail of the striatum (TS) across different species. In rodents, the TS consists of one entity, whereas in tree shrews, cats and non-human primates the TS consists of the tail of the caudate nucleus (CDt) and the posterolateral putamen. (b) Schematic of rodents' TS inputs. The TS receives excitatory afferents (in violet) from a broad range of cortical areas throughout its rostro-caudal extension (from bregma -1.22 mm to -0.94 mm). This includes the frontal association cortex (FrA), motor cortex (M1/2), somatosensory cortex (S1/2), agranular, granular, dysgranular insular cortex (AI/GI/DI), visual cortex (Vis), auditory cortex (Aud), ecto-/peri-/entorhinal cortex (Rhi) and temporal association cortex (Tem). The TS also integrates thalamic inputs arising from the lateral and ventral posterior nuclei (LP and VPM/VPL), medial and lateral geniculate nuclei (MG and LG), mediodorsal nucleus (MD), parafascicular nucleus (PF), posterior intralaminar nucleus (PIL) and pulvinar nucleus. The two main sources of monoaminergic regulation comprise dopaminergic (DA) neurons (in orange) arising from the substantia nigra *pars lateralis* (SNpl) and serotonergic (5-HT) (in turquoise) innervation from the dorsal raphe nucleus (DRN). (c) Schematic of rodents' TS efferents. TS-output neurons are GABAergic SPNs that segregate into two distinct populations projecting either to the caudal part of the external globus pallidus (GPe) (D2R-SPNs or iSPNs) or to the Ep/GPi and SNpr (D1R-SPNs or dSPNs). Schemes have been adapted from the mouse brain atlas [116].

### Figure 2: Identification of distinct domains of the rodent TS.

(a) Schematic cartoon illustrating the TS. Double immunofluorescence of D2R (yellow) and GFP (cyan) in the TS of *Drd2-eGFP* mice. D2R (cyan) immunolabeling in the rat and gerbil

TS. Note the presence in all these species of a longitudinal stripe adjacent to the GPe lacking D2R-expressing SPNs. Scale bar, 200  $\mu$ m. **(b)** Cartoons and list of known markers allowing the delineation of the D2R/A2aR-SPNs-lacking domain (in violet), and the two zones of the D1R- and D2R/A2aR-SPNs-intermingled domain corresponding to the intermediate (in orange) and lateral (in dark grey) parts of the tri-laminar zone [50]. Cx: Cortex; cc: corpus callosum; GPe: external globus pallidus; AST: amygdalostratial transition; CeA: central amygdala, BLA: basolateral amygdala, LA: lateral amygdala; TS: tail of the striatum. Schemes have been adapted from the mouse brain atlas [116].

**Figure 3: Distinct patterns of ERK phosphorylation within the mouse's TS domains.**

**(a)** Double immunofluorescence of pERK (yellow) and TH (cyan) in the TS of C57BL/6 mice 15 min after d-amphetamine (10 mg/kg) administration. Note that d-amphetamine-induced ERK phosphorylation occurs preferentially in the D1R-SPNs of the D2R/A2aR-SPNs-lacking domain. Scale bar, 200  $\mu$ m. High magnification of the area delineated by the white dashed rectangle. Scale bar, 100  $\mu$ m. **(b)** Cartoons summarizing the distinct patterns of ERK phosphorylation induced by a single injection of d-amphetamine (d-amph), MDMA, cocaine, GBR12783 (DAT reuptake inhibitor), methylphenidate and PDE10A inhibitor (papaverine) in the distinct mouse' TS domains. Note that papaverine increases preferentially pERK in D2R-SPNs of the intermediate part of the D1R- and D2R/A2aR-SPNs-intermingled domain. Cx: Cortex; cc: corpus callosum; GPe: external globus pallidus; AST: amygdalostratial transition; LA: lateral amygdala; TS: tail of the striatum. Schemes have been adapted from the mouse brain atlas [116].

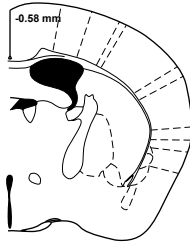
**Table 1. Markers with distinct expression in the medial, intermediate and lateral zones of the TS**

Markers	Zones/Domains	Species	References
SP	medial-enriched	Mouse	[21,35,50]
D1R	intermediate-poor	Mouse, Rat <i>Drd1a-eGFP</i> mice <i>Drd1a-tdTomato</i> mice	[35,47] [35] [47]
TH	intermediate-poor medial-enriched	Mouse, Rat <i>Th-Cre:tdTomato</i> mice	[47,50] [48](Allen Brain Atlas)
CR	medial-enriched	Mouse, rat	[47,50]
D2R	medial-poor	Mouse, Rat, Gerbil <i>Drd2-eGFP</i> , <i>Drd2-Cre:RCE</i> mice <i>Drd2-Cre:RCE</i> or <i>LacZ-TauGFP</i> mice	[47] [35]
A2aR	medial-poor	Mouse, Rat, Gerbil <i>Adora2a-Cre:YFP</i> mice	[47] [35]
PDE1b	medial-poor	<i>Pde1b-Cre</i> mice	[117](Gensat)
Enk	medial-poor	Mouse <i>Penk-2A-CreERT2:tdTomato</i> mice <i>PPE-eGFP</i> mice	[47,50] [48](Allen Brain Atlas) [49]
NT5E	medial-poor	Rat	[51]

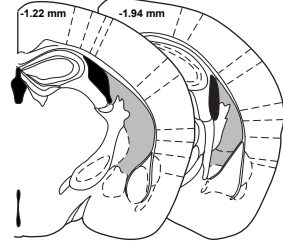
SP: Substance P; D1R: Dopamine D1 receptor; TH: Tyrosine hydroxylase; CR: Calretinin; D2R: Dopamine D2 receptor; A2aR: Adenosine A2a receptor; PDE1b; Phosphodiesterase 1b; Enk; Enkephalin; NT5E; Ecto-5'-nucleotidase

**a** *Mus musculus*

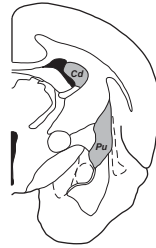
Caudal Striatum



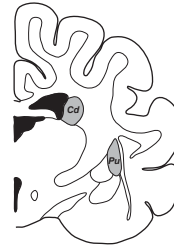
Tail of Striatum



*Tupaia belangeri*



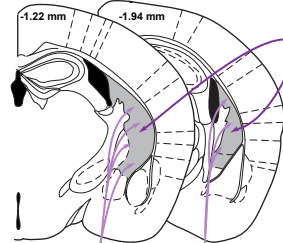
*Felis catus*



*Macaca fascicularis*



**b** Cortico-, Subcortico- and Thalamo-striatal inputs

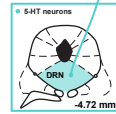
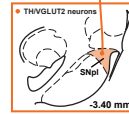
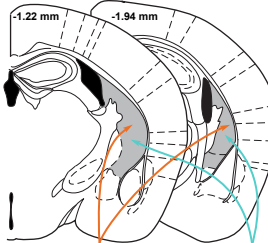


**Subcortical inputs**  
- Amygdala  
- Amygdala  
- Subiculum

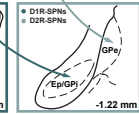
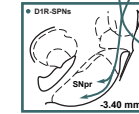
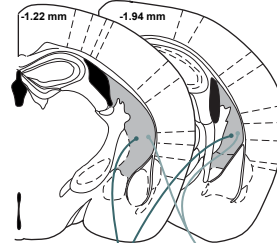
**Cortical inputs**  
- FrA - S1/2  
- M1/2 - AI/GI/DI  
**Thalamic inputs**  
- LP - MD  
- VPM / VPL - PF

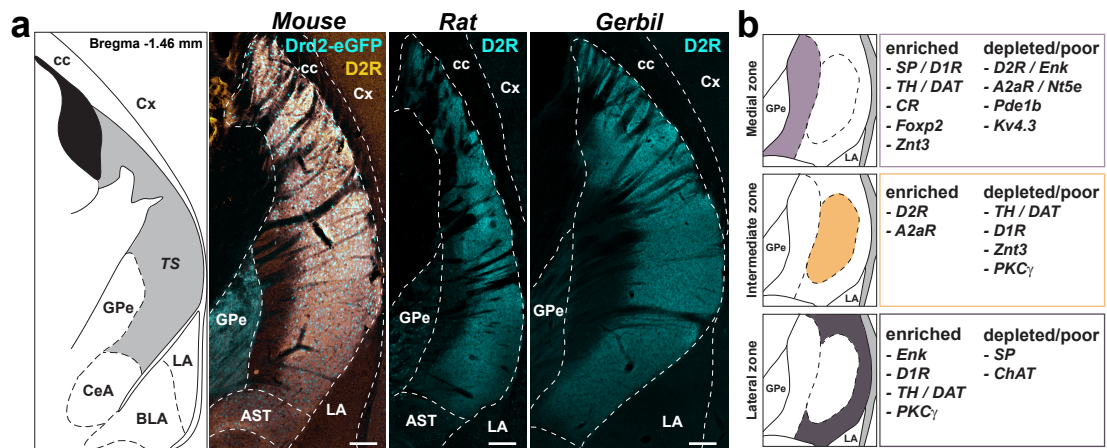
**Cortical inputs**  
- Vis - Rhi  
- Aud - Tem  
**Thalamic inputs**  
- MG / LG - PIL  
- Pulvinar - PF

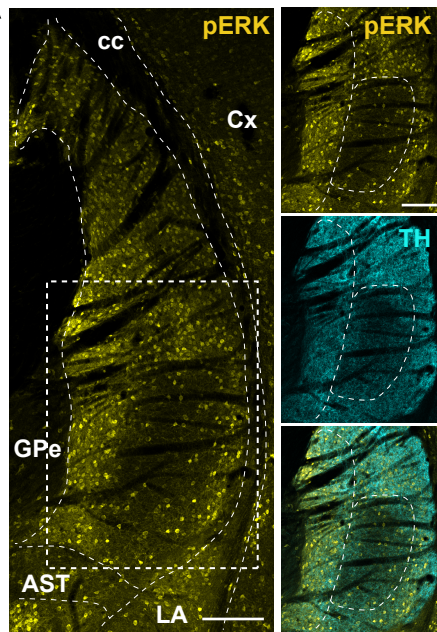
**Monoaminergic inputs**



**c** Outputs





**a****b**